HHS Public Access

Author manuscript

Nat Genet. Author manuscript; available in PMC 2012 October 01.

Published in final edited form as:

Nat Genet. ; 44(4): 406–S1. doi:10.1038/ng.2215.

Generation Of Functional Insulin-Producing Cells In The Gut By Foxo1 Ablation

Chutima Talchai[1,5], **Shouhong Xuan**[2], **Tadahiro Kitamura**[3], **Ronald A. DePinho**[4], and **Domenico Accili**[1]

[1]Berrie Diabetes Center, Department of Medicine, College of Physicians & Surgeons of Columbia University, New York, NY 10032 [2]Berrie Diabetes Center, Department of Genetics and Development, College of Physicians & Surgeons of Columbia University, New York, NY 10032 [3]Metabolic Signal Research Center, Institute for Molecular and Cellular Regulation, Gunma University, Maebashi, Gunma, 371-8512, Japan, [4]Center for Applied Cancer Science, Departments of Medical Oncology, Medicine and Genetics, and Belfer Institute for Innovative Cancer Science, Dana-Farber Cancer Institute, Harvard Medical School, Boston, MA 02115 [5]Faculty of Medicine, King Chulalongkorn Memorial Hospital, Chulalongkorn University, Bangkok, 10330 Thailand

Abstract

Restoration of regulated insulin secretion is the ultimate goal of type 1 diabetes therapy. Here we show that, surprisingly, somatic ablation of *Foxo1* in Neurog3$^+$ enteroendocrine progenitor cells gives rise to gut insulin-positive cells (Ins$^+$) that express markers of mature β-cells, and secrete bioactive insulin as well as C-peptide in response to glucose and sulfonylureas. Lineage tracing experiments show that gut Ins$^+$ cells arise cell-autonomously from Foxo1-deficient cells. Inducible *Foxo1* ablation in adult mice also results in the generation of gut Ins$^+$ cells. Following ablation by the β-cell toxin, streptozotocin, gut Ins$^+$ cells regenerate and produce insulin, reversing hyperglycemia in mice. The data indicate that Neurog3$^+$ enteroendocrine progenitors require active Foxo1 to prevent differentiation into Ins$^+$ cells. *Foxo1* ablation in gut epithelium may provide an approach to restore insulin production in type 1 diabetes.

A longstanding goal of regenerative medicine is the identification of genetic, cellular, and biochemical pathways governing the generation of insulin–producing β-cells, with an eye to enlisting them in ongoing cellular replacement efforts in patients with type 1 diabetes[1,2].

Correspondence should be addressed to D.A. (da230@columbia.edu).

METHODS

Methods and any associated references are available in the online version of the paper at http://www.nature.com/naturegenetics/.

AUTHOR CONTRIBUTIONS

C.T. generated mice, designed and performed experiments and wrote the manuscript. S.X. generated mice and designed experiments. T.K. generated mice and performed immunohistochemistry. R.A.D. designed experiments and wrote the manuscript. D.A. designed experiments and wrote the manuscript.

COMPETING FINANCIAL INTEREST

The authors declare no competing financial interest.

The process by which primitive endodermal precursors adopt an endocrine fate has been examined in detail[3]. A key step appears to be the formation of Neurog3-expressing cells that go on to differentiate into all known pancreatic islet cell types[4-6]. Interestingly, Neurog3$^+$ endocrine progenitors are not restricted to the pancreas, but are found in the stomach and intestine, where they give rise to most cells in the enteroendocrine system, the largest endocrine organ in the body[7,8].

Despite their common endodermal origin, pancreatic and gut Neurog3$^+$ endocrine progenitors share few if any properties: they give rise to cell types that produce distinct peptide hormones, and have remarkably different developmental fates and lifespan[9]. Pancreatic endocrine progenitors are formed during embryonic development, and do not arise again in the adult organ[10], except under special circumstances[11]. Enteroendocrine progenitors instead arise constantly from gut stem cells, and contribute to repopulate the fast-turnover enteroendocrine population[8]. The distinct features of these two cell populations dovetail with the classical theory of positional specification, whereby partly committed progenitor cells acquire position-dependent properties that dictate specific fates[12]. It is unclear how gut Neurog3$^+$ progenitors are restricted to the enteroendocrine *vs*. pancreatic endocrine fate. Understanding this mechanism would allow investigators to explore the use of gut epithelium as a source for cell replacement therapy in insulin-dependent diabetes, given the self-renewing nature of this tissue.

Foxo transcription factors integrate hormonal and nutrient cues with the cell transcriptional response to regulate diverse cellular processes[13]. In addition to their metabolic functions, Foxo proteins inhibit terminal differentiation in multiple cell types[14-16]. In myoblasts, Foxo1 can affect cell fate decisions in a Notch-dependent manner, leading to the generation of different muscle fiber types[17]. In the pancreas, Foxo1 plays an important role to regulate endocrine cell mass[18-20] and β-cell response to oxidative stress [21,22]. Interestingly, Foxo1 is co-expressed with Neurog3 in embryonic pancreas, but Foxo1 ablation does not affect the generation of different pancreatic endocrine cell types[18]. In cultures of human fetal pancreatic epithelium, *FOXO1* knock-down increases the number of *NEUROG3*$^+$ cells[23]. In contrast, virtually nothing is known about functional properties of Foxo1-expressing cells in the gut. In this study, we use a combination of genetic and cellular approaches to answer this question.

RESULTS

Foxo1 ablation expands Neurog3$^+$ enteric progenitors

Foxo1 is expressed in gut epithelial cells, including most Neurog3$^+$ enteroendocrine progenitors (Supplementary Fig. 1a). To investigate its role in this cell type, we generated mice with somatic deletion of *Foxo1* in Neurog3$^+$ cells[8] (*NKO*, or *N*eurog3-Cre-driven Foxo1 *K*nock*O*uts). To assess Cre-mediated recombination, we intercrossed *NKO* and *Neurog3-Gfp* transgenic mice (Supplementary Fig. 1b). Control studies showed that Gfp immunoreactivity co-localizes with endogenous Neurog3 immunoreactivity (Supplementary Fig. 1c). In *NKO* mice, Foxo1 was no longer detectable in Gfp-labeled cells (Supplementary Fig. 1b) and *Foxo1* mRNA decreased > 80% in flow-sorted *Neurog3-Gfp* cells, indicating that the deletion occurred efficiently (Supplementary Fig. 1d). Similar to findings in human

cells following *FOXO1* knock-down[23], *Foxo1* ablation resulted in a tenfold increase in the number of Neurog3$^+$ cells (Fig. 1a), as demonstrated by: (*i*) immunohistochemistry with anti-Neurog3 antibody, (*ii*) lineage tracing studies with either *Neurog3-Gfp* transgenics[10] or (*iii*) *Neurog3-Gfp* knock-in mice[7], (*iv*) flow cytometry analysis of Gfp$^+$ cells derived from *NKO:Neurog3-Gfp* double transgenic mice (Fig. 1b, and Supplementary Fig. 1b-g), and (*v*) *Neurog3* mRNA measurements in flow-sorted Gfp$^+$ cells (Fig. 1c). The increase of Neurog3$^+$ cells was associated with a similar increase of cells expressing Chromogranina A (ChgA) (Fig. 1d,e), a marker of endocrine cell differentiation that is temporally expressed after Neurog3, indicating that Foxo1 ablation expands gut Neurog3$^+$ progenitors and their daughter cells[9]. These data were substantiated by immunohistochemistry with anti-Neurog3 antibodies in large intestine, as well as immunofluorescence with anti-Gfp in adult gut from *Neurog3-Gfp* transgenic and knock-in mice (Supplementary Fig. 1e-h). In addition, it is possible that some epithelial progenitors express low levels of Neurog3 that escape detection by Gfp or immunohistochemistry, yet could produce enough Cre to inactivate Foxo1, leading to further activation of Neurog3.

Neurog3 is physiologically repressed by Notch signaling via Hes1 (ref. 24). The coordinated expansion of Neurog3$^+$ and ChgA$^+$ cells in *NKO* mice phenocopies loss of Notch function in Hes1 knockouts[5,25]. As Foxo1 regulates Hes1 in cooperation with Notch[17], we investigated whether Foxo1 ablation in Neurog3$^+$ progenitors affected Hes1 expression. Indeed, Hes1 protein (Fig. 1f) and mRNA levels (Fig. 1g) were substantilly decreased, as were mRNA levels encoding the Hes-related gene *HesR1*, while *HeyL* was unchanged (Fig. 1g). These data indicate that *Foxo1* ablation inhibits Hes1 expression.

Gut insulin-producing cells in *NKO* mice

Hes1 restricts endocrine plasticity of Neurog3$^+$ progenitors during endodermal development[25,26]. Therefore, we surveyed pancreas and intestines of newborn and adult mice by immunohistochemistry with antibodies against enteric and pancreatic islet hormones. In neonatal *NKO* gut, we made the unexpected finding of pancreatic hormone-producing cells: insulin-immunoreactive cells (Ins$^+$) (Fig. 2a and Supplementary Fig. 2a) and, at lower frequencies, cells immunoreactive with pancreatic glucagon (Gcg$^+$) or pancreatic polypeptide (Ppy$^+$) (Supplementary Fig. 2a). We also observed Ins$^+$ cells throughout the gut of adult mice, primarily in the distal ileum and colon (Supplementary Fig. 2b,c), albeit with lower frequency than in newborns, possibly reflecting the relative expansion of gut epithelial *vs*. enteroendocrine lineages[27]. In addition, we detected *Ins1* and *Ins2* mRNA (Fig. 2b) in small and large intestine, but not in other Neurog3-expressing tissues such as brain, hypothalamus, stomach and testis (Supplementary Fig. 2d).

To investigate the origin of Ins$^+$ cells and provide independent evidence for their identity, we generated additional genetic models in mice. First, we ablated *Foxo1* in duodenal epithelial precursors-the forerunners of Neurog3$^+$ cells–using *Pdx1-Cre*[28] (*P*dx1-Cre-driven Foxo1 *K*nock*O*ut, *PKO*). Crosses of *PKO* mice with *Neurog3-Gfp* reporter mice confirmed Foxo1 ablation (Supplementary Fig. 2e). Similar to *NKO* mice, *PKO* mice showed Ins$^+$ cells in the duodenum, and a marked increase of Neurog3-Gfp$^+$ cells (Supplementary Fig. 2f,g).

These data are consistent with the hypothesis that Foxo1 inhibition in duodenal epithelium precursors is sufficient to generate Ins$^+$ cells.

Next, we generated an *Ins2-Gfp* knock-in allele by gene targeting to provide a sensitive and specific readout of endogenous *Ins2* transcription. When we introduced the *Ins2-Gfp* allele into *NKO* mice, we readily detected Ins2-Gfp$^+$ cells in the gut of mutant mice, but not in WT littermates. In contrast, we detected Ins2-Gfp expression in pancreatic islets of both genotypes (Supplementary Fig. 2h,i). Double immunohistochemistry with either insulin or C-peptide and Gfp antibodies confirmed the identity of Gfp$^+$ cells as Ins$^+$ cells (Fig. 2c and Supplementary Fig. 2j).

Gut Ins$^+$ cells express markers of terminally differentiated insulin-producing cells

We analyzed gut Ins$^+$ cells by immunohistochemistry. In addition to markers shared in common between insulin-producing and enteroendocrine cells, such as synaptophysin (Syp) (Fig. 2d), glucokinase (Gck), and prohormone convertase-1 (Pcsk1) (Supplementary Fig. 2k,l), Ins$^+$ cells expressed markers that are highly enriched in pancreatic β-cells but restricted or absent in the gut: prohormone convertase-2 (Pcsk2)[29] and C-peptide, the enzymatic byproduct of proinsulin processing (Fig. 2d). Furthermore, co-immunostaining revealed that Ins$^+$ cells were distinct from cells producing pancreatic glucagon, Glp1, somatostatin, and Ppy, indicating that they are not mixed-lineage endocrine cells (Fig. 2e and Supplementary Fig. 2a). Quantitative analyses showed that gut Ins$^+$ cells are slightly more frequent than L-cells (Fig. 2f). The morphology of Ins$^+$ cells is conducive to hormone release into the circulation, with narrow apical tips facing the gut lumen, and a wide basal membrane facing blood vessels (Fig. 2d).

To rule out the possibility that gut Ins$^+$ cells arise as a consequence of genetic reprogramming of enteroendocrine precursors caused by *Foxo1* ablation during fetal development, we inactivated *Foxo1* in enteroendocrine progenitors of adult mice using an inducible binary transgenic system. To this end, we intercrossed *Foxo1*$^{lox/lox}$ mice with mice expressing a Tamoxifen (TM)-activatable Cre (*CreER*^{T}) from the *Neurog3* locus[30] to generate *Neurog3*^{CreERT}*KO* mice. We injected 10-wk-old mice with TM or saline and, after two weeks, surveyed intestines for the appearance of Ins$^+$ cells. TM-treated *Neurog3*^{CreERT}*KO* animals showed Ins$^+$/Pcsk2$^+$/C-peptide$^+$ gut cells, whereas WT controls did not (Fig. 2g). These data show that Neurog3$^+$ progenitors require active Foxo1 to repress gut Ins$^+$ fate during intestinal homeostasis in adult animals.

Glucose-dependent release and bioactivity of enteric insulin

Regulated insulin secretion is a critical feature of pancreatic β-cells that has proved difficult to replicate in ES cell-derived insulin-producing cells[2]. To determine whether gut Ins$^+$ cells are functionally competent to secrete insulin, we performed *ex vivo* assays of insulin secretion in response to glucose and K_{ATP} channel modulators, using the vital pancreatic islet dye dithizone (DTZ)[31] to select gut segments enriched in Ins$^+$ cells from *NKO* mice and anatomically matched segments from WT controls. *NKO* intestines released insulin and C-peptide in a glucose dose-dependent manner. The sulfonylurea glibenclamide (a K_{ATP} channel blocker) augmented glucose-induced insulin release, while the K_{ATP} channel opener

diazoxide blunted it (Fig. 3a,b). These findings are consistent with the immunohistochemical analyses indicating that Ins^+ cells possess the relevant sensing proteins: Gck (Fig. 2d), sulfonylurea receptor 1 (Sur1, encoded by *Abcc8*), and glucose transporter 2 (Glut2, encoded by *Scl2a2*) (Supplementary Fig. 3a,b). Thus, functional and histochemical evidence supports the conclusion that gut Ins^+ cells are capable of regulated insulin secretion in response to glucose and K_{ATP} channel modulators.

To examine whether intestinal insulin is bioactive, we prepared acid-ethanol extracts from *NKO* gut, as well as from gut, pancreas and liver of WT mice, and injected them into newborn mice. Extracts from newborn *NKO* intestine lowered blood glucose by ~20%, similar to the reduction achieved by injecting recombinant human insulin (2U/kg), or pancreas extracts from age-matched WT mice. In contrast, extracts from WT intestines or liver had no effect (Fig. 3c). The ability of *NKO* gut extracts to lower blood glucose was preempted by the addition of an insulin-neutralizing antibody, as was that of pancreatic extracts from WT mice and of recombinant insulin, whereas incubating *NKO* gut extracts with isotype-matched control IgG had no effect on their ability to lower glycemia (Fig. 3c), indicating that the hypoglycemic effect is due to insulin and not to other factors in the *NKO* gut extracts. These results show that gut–derived insulin is bioactive.

Regeneration of gut Ins^+ cells following STZ ablation

Unlike pancreatic endocrine cells, enteroendocrine cells arise from $Neurog3^+$ progenitors throughout life[8]. If so, gut Ins^+ cells should have greater regenerative capabilities than islet β-cells in a toxin-induced diabetes model. Streptozotocin (STZ) administration to *NKO* and WT mice resulted in hyperglycemia (Fig. 4a). Glucose levels in WT mice were kept at ~500mg/dL by daily insulin administration for 28 days. In contrast, we held treatment in *NKO* mice. But their glucose levels began to spontaneously decrease nine days post-STZ, and stabilized at ~250 mg/dl in the fed state, consistent with restoration of insulin production (Fig. 4a). Upon insulin withdrawal, 100% of WT mice died, while 75% of *NKO* mice survived until the end of the experiments (Fig. 4b). Moreover, STZ-treated *NKO* mice showed near-normal oral glucose tolerance (Fig. 4c). The improvement could not be ascribed to pancreatic β-cell regeneration, as pancreatic insulin content at the end of experiment was at the lower limits of detection of the assay (< 1 % compared to vehicle-treated controls) (Fig. 4d). We examined gut specimens obtained 3 days after STZ treatment, and Ins^+ cells were undetectable in either genotype (Supplementary Fig. 4a). But at day 28 post-STZ, gut Ins^+ cells were present in *NKO* gut at greater frequency compared to pre-STZ treatment (10.5 *vs*. 4.5%, $P < 0.001$) (Fig. 4e), and expressed markers of mature β-cells: Pcsk2 and C-peptide (Supplementary Fig. 4a,b), suggesting that their functional properties are intact. Moreover, we detected insulin as well as C-peptide 2 in fasted and fed STZ-treated NKO mice using murine-specific ELISA, whereas in WT mice values were at the lower limit of detection (Supplementary Fig. 4c-h). There was no immunohistochemical evidence of pancreatic β-cell regeneration in *NKO* mice, nor of Ins^+ cells in WT gut or pancreas at any stage (Supplementary Fig. 4a). The sensitivity of gut Ins^+ cells to STZ ablation also provides evidence that they are similar to pancreatic β-cells[32].

As Neurog3 is also expressed in the brain[33], we sought to determine a potential contribution from this organ to the observed survival. To this end, we administered STZ to mice with pan-neuronal *Foxo1* ablation (Syn-Cre:*Foxo1*$^{lox/lox}$ or Brain Knock-Out; *BKO*) (Hongxia Ren and Domenico Accili, unpublished observation) and their WT littermates. In either genotype we failed to observe rescue of diabetes (Supplementary Fig. 4i), effectively ruling out a contribution from neuronal Foxo1 ablation to this phenotype.

Derepression of the β–cell program in NKO gut

To probe the identity of gut Ins$^+$ cells, we surveyed expression of pancreatic and intestinal markers. Immunohistochemistry showed that gut Ins$^+$ cells express epithelial markers, such as E-cadherin, but not mesenchymal markers Cd45R, laminin or smooth muscle actin (Sma) (Fig. 5a and Supplementary Fig. 5a-c). This finding indicates that they do not arise in response to epithelial-mesenchymal transition[34]. Moreover, gut Ins$^+$ cells express the insulin gene transcription factor MafA, and MafA$^+$ cells also express pancreatic β-cell transcription factors, Nkx6.1 and Pdx1 (Fig. 5b-d and Supplementary Fig. 5d). In addition, consistent with the presence of cells immunoreactive with pancratic glucagon (Fig. 2e), we detected immunostaining with the α-cell transcription factor, MafB, as well as increased levels of mRNA encoding α– β–cell transcription factors *Pdx1, MafA, Nkx6.1, Nkx2.2, Pax4, Arx*, and *MafB*, but not *NeuroD1* or *Pax6* in gut segments enriched with Ins$^+$ cells (Supplementary Fig. 5e,f).

Development of enteroendocrine L cells is Pax6-dependent[9], while that of Cholecystokinin (Cck) cells is NeuroD1-dependent[35]. Consistent with the normal expression levels of *Pax6* and *NeuroD1*, morphometric analysis of immunostaining data showed that the number of L, Cck–, and Serotonin–producing cells was unchanged in *NKO* mice (Fig 2e,f and Supplementary Fig. 5g). Transcription factor Cdx2 is required for gut endoderm differentiation[36]. Ablation of *Hes1* results in loss of intestinal identity in a sub-population of cells that become transcommitted to the pancreatic fate[25]. In contrast, gut Ins$^+$ cells in *NKO* mice were Cdx2–immunoreactive, indicating that they retain intestinal properties (Fig. 5e). Together these findings provide further evidence that *Foxo1* ablation in *NKO* mice causes derepression of the β–cell (and pancreatic endocrine) program, rather than transdifferentiation of gut epithelium into the pancreatic fate.

Cell-autonomous alterations of Notch and Wnt signaling in gut Ins$^+$ cells

To distinguish whether Ins$^+$ cells arise from cell-autonomous or non-autonomous mechanisms, we performed genetic lineage-tracing experiments. We generated *NKO* mice bearing a *Rosa26eGfp* reporter allele to label Neurog3-Cre–active cells and their daughter cells in adult intestines. In the pancreas, all islet cells were Gfp$^+$ (Fig. 6a). In the *NKO* gut, Ins$^+$ cells were Gfp$^+$, as were C-peptide$^+$ cells (Fig. 6a), indicating that insulin expression occurred in cells that had undergone Cre-mediated recombination. This conclusion was upheld by studies in STZ-treated *NKO:Rosa26eGfp* mice. Similar to the pre-STZ state, Ins$^+$ cells arising after STZ treatment activated endogenous Pcsk2 expression in a cell-autonomous manner (Supplementary Fig. 6a).

Notch and Wnt pathways play critical roles in intestinal epithelial lineage specification[37] and interact with Foxo1[17,38]. To understand whether *Foxo1* ablation affected these pathways, we used low-density array profiling of gut epithelial cell mRNA to identify gene expression changes associated with the appearance of Ins^+ cells in *NKO* mice. In isolated epithelial cells from DTZ-enriched *NKO* gut, we confirmed the substantial downregulation (~7-fold) of *Hes1* observed by immunohistochemistry and qPCR (Fig. 1e,f), thus validating the experimental approach. Whereas some of the Notch-specific genes were downregulated, several transcripts shared in common by Notch and Wnt signaling were upregulated in the Notch and Wnt arrays. Amongst them, we detected a substantial (>300-fold) increase of transcripts encoding the groucho-related gene *Aes* (Amino-terminal enhancer of split, also known as *Tle5* or *Grg5*), and we confirmed it by qPCR analysis[37] (Fig. 6b and Supplementary Fig. 6b,c). We also saw > 3-fold increases in *Fzd1*, *Fzd2*, *Fzd3*, and *Fzd4* (Supplementary Fig. 6c). In contrast to the Notch array, the Wnt array showed upregulation of Wnt ligands, receptors, and transcription factors (Fig. S6c). The corepressor of Polycomb 2-mediated transcription, C-terminal-binding protein 1 (Ctbp1) decreased >1,200-fold (Supplementary Fig. 6c), a finding that might be expected to increase cellular plasticity[39]. These data suggest that *Foxo1* ablation activates Wnt signaling, de-repressing enteroendocrine differentiation pathways, and supporting the notion that Foxo1 inhibits Wnt signaling[16,38].

To link mechanistically the gene expression and cellular differentiation data, we investigated Aes in more detail. Aes is expressed in the pancreas[40] and ectopic Aes expression is associated with expanded Nkx 2.2 and Nkx 6.1 neuronal domains[41]. In addition, Aes is an endogeneous repressor of Notch signaling and Hes1 expression in colon[42]. By immunohistochemistry, we localized Aes expression specifically to Ins^+ cells (Fig. 6c). Accordingly, lineage tracing experiments indicated that Gfp^+ cells in *NKO:Rosa26eGfp* mice were decorated by Aes antibodies (Fig. 6d), demonstrating that Foxo1 ablation promotes Aes expression in a cell-autonomous fashion.

Next, we recapitulated gut Ins^+ cell differentiation *ex vivo*. We isolated intestinal crypts containing $Neurog3^+$ progenitors from mice carrying the *Ins2-Gfp* reporter allele and subjected them to treatment with Wnt3a and Fgf4 to mimic the gene expression findings in PCR arrays from *NKO* mice (Supplementary Fig. 6c). Under these conditions, we observed green fluorescent cells (i.e., Ins2-Gfp^+ cells) in primary cultures from *NKO*, but not WT mice (Fig 6e and Supplementary Fig. 6d).

Using the Wnt3a/Fgf4 induction protocol of primary crypt cultures, we investigated the requirements for Foxo1, Notch/Wnt, and Aes in the generation of Ins^+ cells. Cellular transduction of a constitutively active Foxo1 (ADA) adenovirus confers Foxo1 gain-of-function[15], and would thus be predicted to prevent the generation of Ins2-Gfp^+ cells in cells from *NKO* mice. Indeed, following expression of Foxo1-ADA, the number of Ins2-Gfp^+ cells decreased, while the control (LacZ) adenovirus had no effect (Fig. 6f). Foxo1 is known to interact with Notch through its co-regulatory functions, independent of DNA binding[17]. Accordingly, one could further predict that transduction of a constitutively nuclear DNA binding-deficient Foxo1 (ADA-DBD) would also decrease the number of Ins2-Gfp^+ cells. This too we observed (Fig. 6f). In contrast, isolated Notch inhibition alone, with Compound

E, or isolated Wnt activation with small molecule sc-222416, did not phenocopy Foxo1 inhibition and failed to give rise to Ins2-Gfp$^+$ cells, consistent with the hypothesis that Foxo1 ablation brings about the phenotype by virtue of its combined effects on Notch and Wnt signaling. Finally, we examined the requirement for Aes in this process. When we treated primary crypt cultures with Aes siRNA, the number of Ins2-Gfp$^+$ cells decreased from 0.14% to 0.03% of total (Fig. 6f), whereas a control SiRNA had no effect. These findings were accompanied by the expected changes in *Aes* expression (Supplementary Fig. 6e). The data suggest that Aes is a mediator of the effects of Foxo1 ablation, and that its ectopic expression is necessary for the appearance of Ins2-Gfp$^+$ cells.

DISCUSSION

In this work, we show that fetal and adult ablation of *Foxo1* in enteroendocrine progenitors gives rise to cells with lineage and functional features of insulin-producing, glucose-responsive cells. Functional *ex vivo* data show that gut Ins$^+$ cells release insulin in a glucose-regulated manner and are inhibitable by diazoxide, allaying fears of unchecked insulin release that have plagued cellular replacement approaches to type 1 diabetes. As both pancreatic β-cells and enteroendocrine cells physiologically express Glut2, Gck, and Sur1[43,44], the ability of gut Ins$^+$ cells to secrete insulin might reflect shared glucose-sensing properties between these cell types. There are, however, important differences between Ins$^+$ cells described in this study and enteroendocrine cells, as (*i*) *Foxo1* ablation increases expression of β-cell transcription factors Pdx1, Neurog3, MafA and Nkx6.1, and of the pancreatic endocrine cell-specific terminal differentiation marker, Pcsk2. (*ii*) The observation that Ins$^+$ cells in *NKO* mice express the *Ins2-Gfp* knock-in allele provides evidence of activation of a pancreatic β–cell-like developmental pathway sufficient for glucose-stimulated insulin secretion. (*iii*) Finally, we provide *in vivo* evidence that intestinal insulin is bioactive.

A critical distinguishing feature of gut Ins$^+$ cells from other cell types that have been shown to give rise to Ins$^+$ cells is that gut Ins$^+$ cells can regenerate rapidly following STZ-mediated ablation, unlike ES cells-derived insulin-producing cells[2,45]. As Ins$^+$ gut cells in untreated *NKO* mice and post-STZ express similar markers of mature β-cells (Pcsk2) and active Wnt signaling (Aes), we speculate that they arise from similar developmental programs.

The morphology of gut Ins$^+$ cells (Fig. 2d) is consistent with the possibility that they secrete insulin in response to bloodborne, rather than gut lumenal cues. Gut Ins$^+$ cells are not arrayed into islet-like structures, but neither are other enteroendocrine cells, possibly reflecting spatial and temporal constraints.

Lineage tracing data indicate that Ins$^+$ cells arise in a cell-autonomous manner from Foxo1-deficient Neurog3$^+$ progenitors, as do Gcg$^+$ and Ppy$^+$ cells, albeit at commensurately lower frequencies, suggesting that the entire pancreatic endocrine lineage is derepressed by *Foxo1* ablation. This property is loosely reminiscent of the ability of other forkhead proteins to repress mesenchymal fate in neural crest progenitors[46], or the testis-specific enhancer, Sox9, in ovaries[47]. This finding suggests that in normal development and intestinal homeostasis,

Foxo1 acts as a cell-autonomous suppressor of the pancreatic endocrine fate in Neurog3$^+$ progenitors (Supplementary Fig. 7).

We provide evidence that *Foxo1* ablation converts gut Neurog3$^+$ progenitors into progenitors of gut and pancreatic endocrine lineages through altered Notch (decreased Hes1) and Wnt signaling (increased Aes), both of which have been shown to regulate gut and pancreatic differentiation and to interact with Foxo[17,38]. The effect of Foxo1 ablation to steer enteroendocrine Neurog3$^+$ progenitors toward the pancreatic endocrine lineage cannot be ascribed solely to Neurog3 gain-of-function, because only a fraction of Neurog3$^+$ cells become Ins$^+$. Moreover, Neurog3 overexpression is not sufficient to yield Ins$^+$ cells[48].

In a broader context, regulation of enteroendocrine plasticity highlighted by our findings could play an important role in the metabolic functions of the gut[49]. And the ability of NKO mice to regenerate gut Ins$^+$ cells following STZ treatment suggests that pharmacological or RNA-based Foxo1 inhibition in the gut will improve prospects of cell-based therapies to replace insulin administration in type 1 diabetes.

Supplementary Material

Refer to Web version on PubMed Central for supplementary material.

ACKNOWLEDGMENTS

Supported by grants from the NIH (DK58282, DK64819), the Columbia University Diabetes Research Center (DK63608), the Druckenmiller Fellowship of the New York Stem Cell Foundation, the Brehm Coalition, and the Russell Berrie Foundation. We thank Drs. A. Efstratiadis for Ins2-Gfp knock-in mice, A. Leiter for Neurog3-Cre mice, L. Sussel, J.Y. Kim-Muller, and T. Mastracci for advice and reagents, and Q. Xu for technical support. We thank members of the Accili laboratory for insightful discussion and critical reading of the manuscript.

APPENDIX

ONLINE METHODS

Antibodies and immunohistochemistry

We performed tissue fixation and processing for immunohistochemistry as described[19]. We used the rabbit primary antibodies to Foxo1, Pcsk1, and Glucokinase (Santa Cruz), Pdx1 (gift from C. Wright), Cholecystokinin (Aviva System Biology), Laminin (Abcam), Serotonin (Novus Biologicals), C-peptide, glucagon, Glp1, Pancreatic polypeptide, (Phoenix Peptide), GFP (Invitrogen), ChgA, Glut2 (Chemicon), PC2 (US Biologicals), MafA, MafB (Bethyl Laboratories); guinea pig primary antibodies to insulin (Dako), Pancreatic-peptide (Linco), mouse primary antibody to glucagon, Actin, α-Smooth Muscle, (Sigma), Cd45R, E-cadherin (BD Bioscience), Cdx2 (Biogenex), Neurog3 (Developmental Studies Hybridoma Bank) and Synaptophysin (Millipore), and goat primary antibodies to GFP (Rockland), Nkx6.1, Sur1, TLE5/Aes, Neurog3 (Santa Cruz), and Pdx1 (from C. Wright). For Hes1 staining, we used rat primary antibody HES-1 (MBL international) and TSA-HRP amplification kit (Invitrogen) as described[50]. We used FITC, Cy3-, and Alexa-conjugated donkey secondary antibodies (Jackson Immunoresearch Laboratories, and Molecular Probes Inc), or peroxidase staining as described. We stained nuclei with DAPI or DRAQ5 (Cell

Signaling), acquired and analyzed images as described[19]. We obtained images of immunoflorescent colocalization using confocal microscopy (Zeiss LSM 510). Gut morphometric analysis was sampled from 4 sections 150 μM apart and we counted at least 1,000 $ChgA^+$ cells per mouse.

Animals

Pdx1-Cre[28], Neurog3-Cre[8], Rosa26-eGfp, Neurog3-Gfp[10], and *Neurog3*^{CreERT} (Ref. 30) have been described. 4-hydroxytamoxifen (4HT; SIGMA) was used to activate recombination by Cre^{ERT}. We intercrossed them with *Foxo1*$^{flox/+}$ mice[51] to generate *Neurog3-cre:Foxo1*$^{lox/lox}$(*NKO*) and *Pdx1-cre:Foxo1*$^{lox/lox}$(*PKO*). To generate *Ins2-Gfp* knock-in mice, we modified BAC clone RP22-342 (CHORI, Oakland, CA) by recombineering to replace the *Ins2* coding sequence with Gfp. We transfected recombinant clones in ES cells, and selected homologous recombinants by Southern blotting. We generated germ-line chimeras as described previously[52].

Physiological studies

We induced diabetes by intraperitoneal injection of streptozotocin (STZ) (325 mg/kg) into 8-10 month-old mice. Only mice with blood glucose higher than 500mg/dL at post-STZ day 3 were used for further experiments. We treated control mice with daily injections of 2-4 U of NPH-insulin (Eli Lilly). We measured fed glucose and insulin, and C-peptide 2 by ELISA (Millipore) as described[52].

Insulin bioassay

We prepared acid-ethanol extracts from neonatal (P3) gut, liver, and pancreas[53]. We mixed tissue extract or recombinant human Insulin (Humulin R, Eli Lilly) in acid-ethanol with either insulin neutralizing antibody (Thermo Scientific) or isotype-matched mouse IgG1 (Ebiosciences) for subcutaneous injections in 2U per kg body weight. We measured glucose immediately prior to and 5 minutes after injections.

Insulin secretion and content

We stained adult intestine in medium containing 0.12 mM Dithizone (DTZ)[31] and selected 5–inches–long DTZ^+ fragments from *NKO* mice or anatomically matched fragments from control WT mice. We made *en face* preparations of the intestines and incubated them in Krebs Ringer buffer (Sigma) supplemented with glucose at various concentrations, diazoxide (Sigma), or glibenclamide (Tocris) for 1hr. At the end of the incubation, we measured insulin and C-peptide 2 content in the medium by ELISA (Millipore). Collagenase-purified pancreatic islets from 14-week-old WT mice served as controls[18]. Pancreatic insulin contents were extracted by acid ethanol[53], and measured by ELISA.

Isolation of gut epithelial cells

We dissected intestines *en face*, washed them with PBS (Mg^{2+}/Ca^{2+}), minced them into 5 to 10 mm-long pieces, and incubated them in 20 mM EDTA at 37 C followed by vigorous resuspension in cold PBS. We then collected the released epithelial cells for secretion and

RNA assays. We carried out single cell isolation of gut epithelium for FACS analysis as described, except that we included villi fractions[27].

Primary gut culture

We seeded cells in 1:5 dilution of Matrigel (BDbioscience)[54] and incubated overnight in basal media, modified to include anti-mEGF (20ng/mL), insulin from bovine pancreas, hydrocortisone-21-hemisuccinate sodium salt (150nM) (all from Sigma), N2 and B27 supplement (R&D system), 2% Fetal Calf Serum (Hyclone; Thermo Scientific). Cultures were then transferred to either basal or advanced media that include Chir99021 (6μM) and LDN-193189 (Stemgent) plus the following recombinant proteins alone or in combination: m-Wnt3a, m-Wnt5b, R-spondin, Noggin, Fgf4 (200 ng/mL) for 4 days. We prepared smartpool Aes and control siRNA as indicated by manufacture protocol (Themo Scientific). We carried out adenoviral transduction as described[17]. Notch inhibitor, Compound E (EMD Calbiochem) and Wnt agonist (Santa Cruz; sc222416) were applied at 1nM, and 100 μM, respectively.

RNA procedures

We used standard techniques for mRNA isolation and quantitative PCR. Primer sequences for Pcsk2, Gck, Kir6.2, Sur1, Neurog3, Pdx1, MafA, MafB, Nkx6.1, NeuroD1, Nkx2.2,Arx, Pax4, Pax6, Hprt, Tubulin2 (Ref. 55), *Ins1, Ins2* (Ref. 56), *Foxo1, Hes1* (Ref. 17) and *Aes* (SABioscience) have been described. cDNAs for mouse Notch and Wnt Signaling were prepared according to low-density PCRArray manufacture protocol (SABioscience).

Statistical analysis

We analyzed data using Student's t-test. We present data as means ± SEM.

References

1. Zhou Q, Melton DA. Pathways to new beta cells. Cold Spring Harb Symp Quant Biol. 2008; 73:175–81. [PubMed: 19478324]
2. Kroon E, et al. Pancreatic endoderm derived from human embryonic stem cells generates glucose-responsive insulin-secreting cells in vivo. Nat Biotechnol. 2008; 26:443–52. [PubMed: 18288110]
3. Bonal C, Herrera PL. Genes controlling pancreas ontogeny. Int J Dev Biol. 2008; 52:823–35. [PubMed: 18956314]
4. Gradwohl G, Dierich A, LeMeur M, Guillemot F. neurogenin3 is required for the development of the four endocrine cell lineages of the pancreas. Proc Natl Acad Sci U S A. 2000; 97:1607–1611. [PubMed: 10677506]
5. Jensen J, et al. Control of endodermal endocrine development by Hes-1. Nat Genet. 2000; 24:36–44. [PubMed: 10615124]
6. Schwitzgebel VM, et al. Expression of neurogenin3 reveals an islet cell precursor population in the pancreas. Development. 2000; 127:3533–42. [PubMed: 10903178]
7. Lee CS, Perreault N, Brestelli JE, Kaestner KH. Neurogenin 3 is essential for the proper specification of gastric enteroendocrine cells and the maintenance of gastric epithelial cell identity. Genes Dev. 2002; 16:1488–97. [PubMed: 12080087]
8. Schonhoff SE, Giel-Moloney M, Leiter AB. Neurogenin 3-expressing progenitor cells in the gastrointestinal tract differentiate into both endocrine and non-endocrine cell types. Dev Biol. 2004; 270:443–54. [PubMed: 15183725]

9. Schonhoff SE, Giel-Moloney M, Leiter AB. Minireview: Development and differentiation of gut endocrine cells. Endocrinology. 2004; 145:2639–44. [PubMed: 15044355]
10. Gu G, Dubauskaite J, Melton DA. Direct evidence for the pancreatic lineage: NGN3+ cells are islet progenitors and are distinct from duct progenitors. Development. 2002; 129:2447–2457. [PubMed: 11973276]
11. Xu X, et al. Beta cells can be generated from endogenous progenitors in injured adult mouse pancreas. Cell. 2008; 132:197–207. [PubMed: 18243096]
12. Hunt RK, Jacobson M. Specification of positional information in retinal ganglion cells of Xenopus: stability of the specified state. Proc Natl Acad Sci U S A. 1972; 69:2860–4. [PubMed: 4507610]
13. Accili D, Arden KC. FoxOs at the crossroads of cellular metabolism, differentiation, and transformation. Cell. 2004; 117:421–6. [PubMed: 15137936]
14. Hribal ML, Nakae J, Kitamura T, Shutter JR, Accili D. Regulation of insulin-like growth factor-dependent myoblast differentiation by Foxo forkhead transcription factors. J Cell Biol. 2003; 162:535–41. [PubMed: 12925703]
15. Nakae J, et al. The forkhead transcription factor Foxo1 regulates adipocyte differentiation. Dev Cell. 2003; 4:119–29. [PubMed: 12530968]
16. Paik JH, et al. FoxOs cooperatively regulate diverse pathways governing neural stem cell homeostasis. Cell Stem Cell. 2009; 5:540–53. [PubMed: 19896444]
17. Kitamura T, et al. A Foxo/Notch pathway controls myogenic differentiation and fiber type specification. J Clin Invest. 2007; 117:2477–85. [PubMed: 17717603]
18. Kitamura T, et al. Regulation of pancreatic juxtaductal endocrine cell formation by FoxO1. Mol Cell Biol. 2009; 29:4417–30. [PubMed: 19506018]
19. Kitamura T, et al. The forkhead transcription factor Foxo1 links insulin signaling to Pdx1 regulation of pancreatic beta cell growth. J Clin Invest. 2002; 110:1839–47. [PubMed: 12488434]
20. Okamoto H, et al. Role of the forkhead protein FoxO1 in beta cell compensation to insulin resistance. J Clin Invest. 2006; 116:775–82. [PubMed: 16485043]
21. Kawamori D, et al. The forkhead transcription factor Foxo1 bridges the JNK pathway and the transcription factor PDX-1 through its intracellular translocation. J Biol Chem. 2006; 281:1091–8. [PubMed: 16282329]
22. Kitamura YI, et al. FoxO1 protects against pancreatic beta cell failure through NeuroD and MafA induction. Cell Metab. 2005; 2:153–63. [PubMed: 16154098]
23. Al-Masri M, et al. Effect of forkhead box O1 (FOXO1) on beta cell development in the human fetal pancreas. Diabetologia. 2010; 53:699–711. [PubMed: 20033803]
24. Lee JC, et al. Regulation of the pancreatic pro-endocrine gene neurogenin3. Diabetes. 2001; 50:928–36. [PubMed: 11334435]
25. Fukuda A, et al. Ectopic pancreas formation in Hes1 -knockout mice reveals plasticity of endodermal progenitors of the gut, bile duct, and pancreas. The Journal of clinical investigation. 2006; 116:1484–93. [PubMed: 16710472]
26. Kageyama R, Ohtsuka T, Tomita K. The bHLH gene Hes1 regulates differentiation of multiple cell types. Molecules and cells. 2000; 10:1–7. [PubMed: 10774739]
27. van der Flier LG, Clevers H. Stem cells, self-renewal, and differentiation in the intestinal epithelium. Annu Rev Physiol. 2009; 71:241–60. [PubMed: 18808327]
28. Hingorani SR, et al. Preinvasive and invasive ductal pancreatic cancer and its early detection in the mouse. Cancer Cell. 2003; 4:437–50. [PubMed: 14706336]
29. Fujita Y, et al. Glucose-dependent insulinotropic polypeptide is expressed in pancreatic islet alpha-cells and promotes insulin secretion. Gastroenterology. 2010; 138:1966–75. [PubMed: 20138041]
30. Wang S, et al. Sustained Neurog3 expression in hormone-expressing islet cells is required for endocrine maturation and function. Proceedings of the National Academy of Sciences of the United States of America. 2009; 106:9715–20. [PubMed: 19487660]
31. Tuttle RL, et al. Regulation of pancreatic beta-cell growth and survival by the serine/threonine protein kinase Akt1/PKBalpha. Nat Med. 2001; 7:1133–7. [PubMed: 11590437]
32. Nielsen K, et al. Beta-cell maturation leads to in vitro sensitivity to cytotoxins. Diabetes. 1999; 48:2324–32. [PubMed: 10580420]

33. Sommer L, Ma Q, Anderson DJ. neurogenins, a novel family of atonal-related bHLH transcription factors, are putative mammalian neuronal determination genes that reveal progenitor cell heterogeneity in the developing CNS and PNS. Molecular and cellular neurosciences. 1996; 8:221–41. [PubMed: 9000438]
34. Gershengorn MC, et al. Epithelial-to-mesenchymal transition generates proliferative human islet precursor cells. Science. 2004; 306:2261–4. [PubMed: 15564314]
35. Naya FJ, et al. Diabetes, defective pancreatic morphogenesis, and abnormal enteroendocrine differentiation in BETA2/neuroD-deficient mice. Genes Dev. 1997; 11:2323–2334. [PubMed: 9308961]
36. Gao N, White P, Kaestner KH. Establishment of intestinal identity and epithelial-mesenchymal signaling by Cdx2. Developmental cell. 2009; 16:588–99. [PubMed: 19386267]
37. Nakamura T, Tsuchiya K, Watanabe M. Crosstalk between Wnt and Notch signaling in intestinal epithelial cell fate decision. J Gastroenterol. 2007; 42:705–10. [PubMed: 17876539]
38. Essers MA, et al. Functional interaction between beta-catenin and FOXO in oxidative stress signaling. Science. 2005; 308:1181–4. [PubMed: 15905404]
39. Sewalt RG, Gunster MJ, van der Vlag J, Satijn DP, Otte AP. C-Terminal binding protein is a transcriptional repressor that interacts with a specific class of vertebrate Polycomb proteins. Molecular and cellular biology. 1999; 19:777–87. [PubMed: 9858600]
40. Hoffman BG, Zavaglia B, Beach M, Helgason CD. Expression of Groucho/TLE proteins during pancreas development. BMC Dev Biol. 2008; 8:81. [PubMed: 18778483]
41. Muhr J, Andersson E, Persson M, Jessell TM, Ericson J. Groucho-mediated transcriptional repression establishes progenitor cell pattern and neuronal fate in the ventral neural tube. Cell. 2001; 104:861–73. [PubMed: 11290324]
42. Sonoshita M, et al. Suppression of colon cancer metastasis by Aes through inhibition of Notch signaling. Cancer Cell. 2011; 19:125–37. [PubMed: 21251616]
43. Cheung AT, et al. Glucose-dependent insulin release from genetically engineered K cells. Science. 2000; 290:1959–62. [PubMed: 11110661]
44. Nielsen LB, et al. Co-localisation of the Kir6.2/SUR1 channel complex with glucagon-like peptide-1 and glucose-dependent insulinotrophic polypeptide expression in human ileal cells and implications for glycaemic control in new onset type 1 diabetes. Eur J Endocrinol. 2007; 156:663–71. [PubMed: 17535866]
45. D'Amour KA, et al. Production of pancreatic hormone-expressing endocrine cells from human embryonic stem cells. Nat Biotechnol. 2006; 24:1392–401. [PubMed: 17053790]
46. Mundell NA, Labosky PA. Neural crest stem cell multipotency requires Foxd3 to maintain neural potential and repress mesenchymal fates. Development. 2011
47. Uhlenhaut NH, et al. Somatic sex reprogramming of adult ovaries to testes by FOXL2 ablation. Cell. 2009; 139:1130–42. [PubMed: 20005806]
48. Bjerknes M, Cheng H. Neurogenin 3 and the enteroendocrine cell lineage in the adult mouse small intestinal epithelium. Dev Biol. 2006; 300:722–35. [PubMed: 17007831]
49. Drucker DJ. The biology of incretin hormones. Cell Metab. 2006; 3:153–65. [PubMed: 16517403]
50. Ridgway J, et al. Inhibition of Dll4 signalling inhibits tumour growth by deregulating angiogenesis. Nature. 2006; 444:1083–7. [PubMed: 17183323]
51. Paik JH, et al. FoxOs Are Lineage-Restricted Redundant Tumor Suppressors and Regulate Endothelial Cell Homeostasis. Cell. 2007; 128:309–23. [PubMed: 17254969]
52. Okamoto H, et al. Transgenic rescue of insulin receptor-deficient mice. J Clin Invest. 2004; 114:214–23. [PubMed: 15254588]
53. Sherman BM, Gorden P, Roth J, Freychet P. Circulating insulin: the proinsulin-like properties of "big" insulin in patients without islet cell tumors. J Clin Invest. 1971; 50:849–58. [PubMed: 4323127]
54. Golaz JL, Vonlaufen N, Hemphill A, Burgener IA. Establishment and characterization of a primary canine duodenal epithelial cell culture. In Vitro Cell Dev Biol Anim. 2007; 43:176–85. [PubMed: 17577610]

55. Gao N, et al. Foxa2 controls vesicle docking and insulin secretion in mature Beta cells. Cell Metab. 2007; 6:267–79. [PubMed: 17908556]

56. Suzuki A, Nakauchi H, Taniguchi H. Glucagon-like peptide 1 (1-37) converts intestinal epithelial cells into insulin-producing cells. Proc Natl Acad Sci U S A. 2003; 100:5034–9. [PubMed: 12702762]

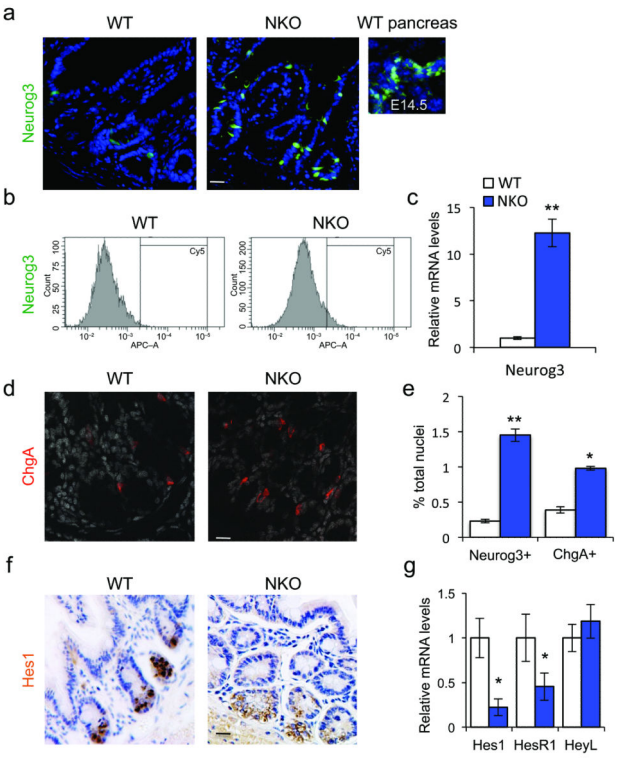

Figure 1.

Foxo1 ablation in enteroendocrine progenitors expands the pool of Neurog3^{+} cells. (**a**) Neurog3 immunohistochemistry (green) in small intestines of adult WT or NKO mice or in pancreas from developmental day E14.5. (**b**) Flow cytometry profiles of gut epithelial cell preparations isolated from WT or NKO mice. (**c**) qPCR analysis of *Neurog3* expression in isolated epithelial cells from small and large intestines of *NKO* (blue bars) or control (white bars) mice. (**d**) ChgA immunostaining (red) in adult large intestines. (**e**) Hes1 immunoreactivity (brown) in adult large intestines. (**f**) Quantification of gut cells reactive with antibodies to Neurog3 or ChgA, a pan-endocrine marker, by flow cytometry analysis. (**g**) qPCR analysis of *Hes1*, *HesR1*, *and HeyL* expression in isolated epithelial cells from small and large adult intestines. Scale bars: 40 μm (a, f), 30 μm (d), (n = 3 for histology n=4 for flow cytometry, and n = 8 for qPCR). * = $P < 0.05$, ** = $P < 0.01$. Error bars indicate SEM.

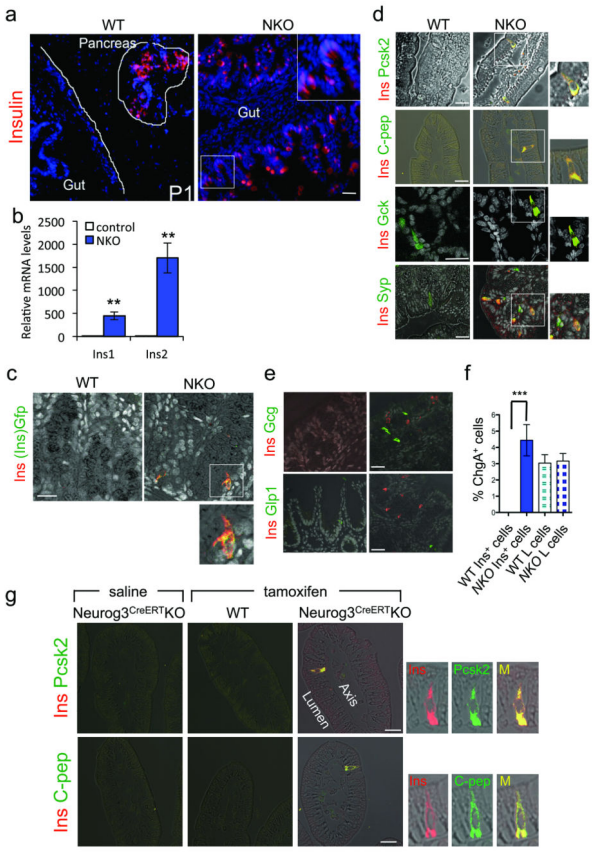

Figure 2.

Gut insulin–producing cells in *NKO* mice. (**a**) Insulin immunohistochemistry (red) in pancreas (outlined) and small intestine of 1-day-old mice. (**b**) qPCR analysis of *Ins1* and *Ins2* expression in isolated epithelial cells from DTZ-enriched gut fragments in *NKO* mice (blue bars) and anatomically matched segments in control mice (white bars). (**c**) Immunofluorescence with insulin (red) and Gfp (green) in *NKO:Ins2-Gfp* mice. (**d**) Co-localization of insulin (red) and the following markers: Prohormone convertase 2 (Pcsk2), C-peptide, Glucokinase (Gck), and Synaptophysin (Syp) (all in green) in adult intestines. (**e**) Immunostaining with insulin (red), and glucagon (Gcg), or glucagon-like peptide-1 (Glp1) (green). (**f**) Morphometric analysis of gut Ins^+ and L cells from distal ileum and colon in 3-month-old mice normalized by total number of $ChgA^+$ cells. Error bars indicate SEM. (**g**) Tamoxifen-induced Foxo1 deletion in adult mice with *Neurog3-Cre^{ERT}*. Panels show co-immunolocalization of insulin (red) with either Pcsk2 or C-peptide (green), two weeks after saline (left panels) or tamoxifen (TM) injection (middle and right panels) in 10-wk-old *Neurog3^{CreERT}KO* and controls. Scale bars: 100 μm (a), 40 μm (e), and 30 μm (c-d, g) (n = 3 for histology and n = 8 for qPCR). * = $P < 0.05$, ** = $P < 0.01$, *** = $P < 0.001$.

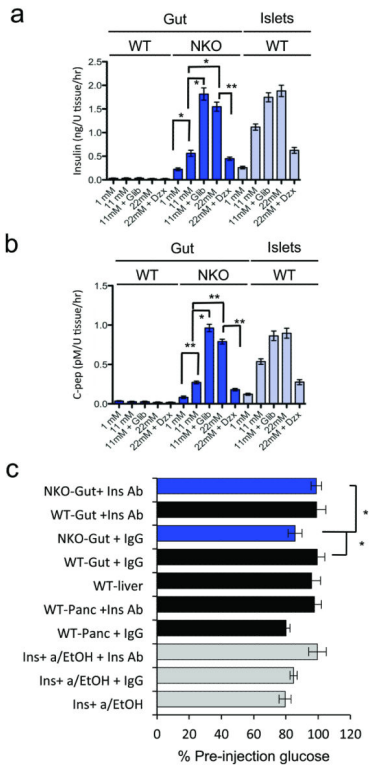

Figure 3.

Insulin secretion and bioactivity. (**a, b**) Glucose-dependent insulin and C-peptide secretion from *NKO* (blue bars) and control gut or islets (gray bars) of adult mice incubated with the indicated concentrations of glucose and 0.5 mM diazoxide (Dzx), or 10 nM Glibenclamide (Glib) (n = 4). U tissue corresponds to 1-inch of gut or one islet. (**c**) Effects of acid-ethanol extracts from *NKO* (blue bars) or control mice (gray bars) on glucose levels following subcutaneous injections in 5-day-old mice. Samples were pre-incubated with anti-insulin neutralizing antibody (Ins Ab), or isotype-matched control IgG (IgG). Recombinant human insulin (2U per kg body weight) was subjected to acid-ethanol precipitation prior to injection (acid/EtOH) (n = 8 in a-b, and n = 12 in c). 3 independent experiments were performed for secretion assays and 2 for bioassay. * = $P < 0.05$, ** = $P < 0.01$. Error bars indicate SEM.

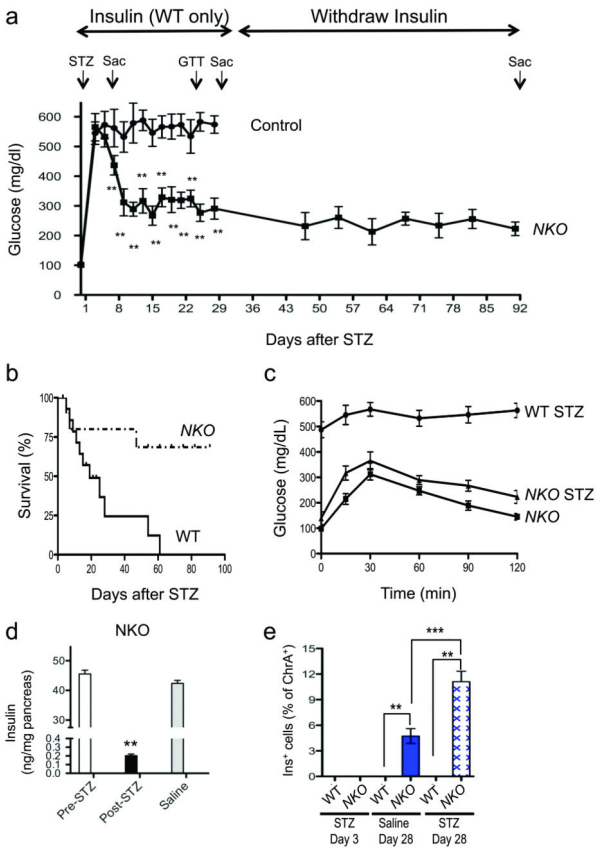

Figure 4.

Regeneration of gut Ins$^+$ cells following STZ-mediated ablation. (**a**) Fed glucose levels in *NKO* (squares) and control mice (circles). Arrows indicate timing of STZ administration (STZ) and killing (SAC). Insulin (2-4 U/kg/day) was administered to control mice from day 3 to day 28 (n = 16). (**b**) Survival plots of *NKO* and WT mice following STZ. (**c**) Oral glucose tolerance tests in *NKO* mice before and after STZ administration (day 20), and in WT controls following STZ (day 20). (**d**) Pancreatic insulin content of *NKO* mice pre- or post-STZ (black bar), or saline injection (n = 4). (**e**) Quantification of gut Ins$^+$ cells in WT and *NKO* mice at day 3 and day 28 post-injection, in animals treated with saline (blue bar), or STZ (hatched pattern). * = $P < 0.05$, ** = $P < 0.01$, *** = $P < 0.001$. Error bars indicate SEM.

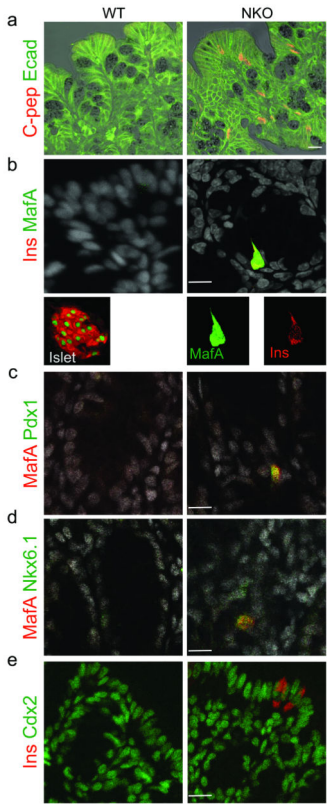

Figure 5.

Marker analysis of gut Ins^{+} cells. (**a**) Immunohistochemical co-localization of E-cadherin (green) and C-peptide (red). (**b**) Co-localization of β-cell transcription factor MafA (red) with insulin (green) in gut and islets. In the gut, the antigen retrieval procedure for co-immunostaining leads to cytoplasmic bleed-through of MafA immunoreactivity. (**c-d**) Co-localization of MafA (red) with β-cell transcription factors Pdx1 or Nkx6.1 (green). (**e**) Co-localization of insulin (red) with Cdx2 (green). Images were taken from colon and distal ileum of adult *NKO* and WT mice. Scale bars: 30 μm (a-e) n=4.

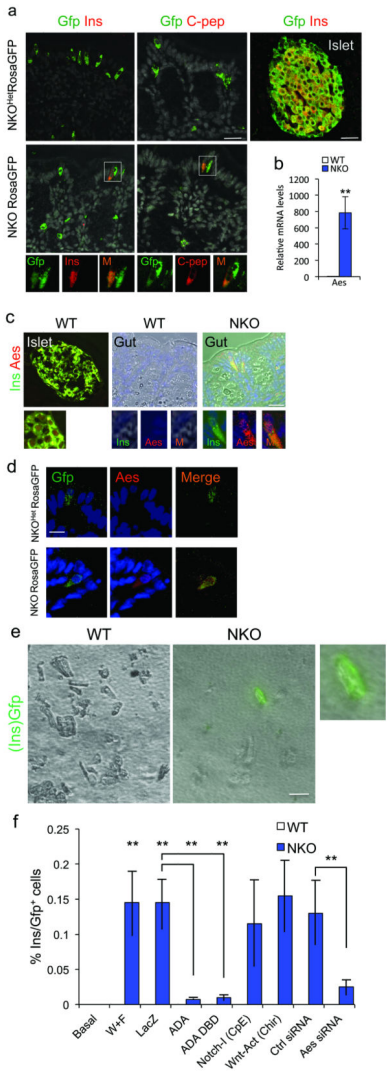

Figure 6.

Lineage tracing of Ins$^+$ cells and Aes expression. (**a**) Immunohistochemistry with Gfp (green) and insulin or C-peptide (red) in WT islets, WT gut, and *NKO:Rosa26eGfp* gut. Gfp$^+$/Ins$^+$ or Gfp$^+$/C-peptide$^+$ cells are indicated in rectangles. (**b**) qPCR of gut *Aes* mRNA sampled from gut segments enriched with Ins$^+$ cells and anatomically matched specimens from WT controls (n=4). (**c**) Islet and gut immunohistochemistry with insulin (green) and Aes (red) in *NKO* and control mice. (**d**) Gut immunostaining with Gfp (green) and Aes (red) in *NKO:Rosa26eGfp* and WT mice. (**e**) Gfp direct fluorescence of primary gut cells isolated from *NKO:Ins2-Gfp or Ins2-Gfp* control mice and cultured in Wnt3a- and Fgf4-containing medium for 4 days. (**f**) Quantification of *Ins2-Gfp* cells in differentiation assays. With the exception of basal conditions, all treatments included Wnt3a and Fgf4 (W+F), and were further subjected to viral transduction (LacZ, Foxo1-ADA, or Foxo1-DBD-ADA), or Notch inhibitor (Compound E), or Wnt agonist (sc222416), or siRNA. No Gfp$^+$ cells from *Ins2-Gfp* control mice were observed in any condition (white bars). Blue bars indicate counts of Gfp$^+$ cells in cultures from *NKO:Ins2-Gfp* mice. Data indicate means ± SEM from 3

independent experiments. Scale bars: 40 μm (a, c), 30 μm (e), and 20 μm (d). * = $P < 0.05$, ** = $P < 0.01$.